Sensors & Actuators: B. Chemical 432 (2025) 137460

Contents lists available at ScienceDirect

Sensors and Actuators: B. Chemical

journal homepage: www.elsevier.com/locate/snb

Unlocking the potential of NH_2-MIL-101 (Fe) nanoMOF for advanced electrochemical immunosensing in chronic wound diagnostics

Víctor Pérez-Ginés [a,b], David Valero-Calvo [a,c], Rebeca M. Torrente-Rodríguez [b], María Pedrero [b], Francisco J. García-Alonso [c,d], José M. Pingarrón [b], Susana Campuzano [b,*], Alfredo de la Escosura-Muñiz [a,c,**]

[a] NanoBioAnalysis Group-Department of Physical and Analytical Chemistry, University of Oviedo, Julián Clavería 8, Oviedo 33006, Spain
[b] Electroanalysis and Electrochemical (Bio)sensors Group, Department of Analytical Chemistry, Faculty of Chemical Sciences, Complutense University of Madrid, Madrid 28040, Spain
[c] Biotechnology Institute of Asturias, University of Oviedo, Santiago Gascon Building, Oviedo 33006, Spain
[d] NanoBioAnalysis Group-Department of Organic and Inorganic Chemistry, University of Oviedo, Julián Clavería 8, Oviedo 33006, Spain

ARTICLE INFO

Keywords:
Chronic wound
Diagnostics
Metal-organic framework
NanoMOF
Electrochemical biosensor
Magnetic beads

ABSTRACT

In this work we take advantage, for the first time, of the porous and functional structure of a nanoscale metal organic framework (nanoMOF), specifically NH_2-MIL-101 (Fe) nanoMOF, for its use as advantageous enzyme-carrier nanotag in immunoassays. In particular, the porous structure of the nanoMOF allows accommodating a high loading of enzyme molecules, which, in addition, are protected from degradation inside the pores providing a high stability. This property together with the ability of the nanoMOF to link antibodies through its functional groups make it a very robust and powerful label. Both the enhanced sensitivity, compared with the conventional use of enzyme-labelled antibodies, and the high long-term stability are demonstrated. Such nanotag also offers advantages related to ease of modification and cost effectiveness. The detection of myeloperoxidase (MPO), a key biomarker for chronic wound monitoring, is proposed to demonstrate the applicability of this approach. A sandwich-type immunoassay using magnetic beads (MBs)-based platforms and subsequent amperometric detection allows the determination of MPO in the clinical range (5 – 100 ng mL^{-1}), with a limit of detection of 1.4 ng mL^{-1}, and good reproducibility ($RSD_{(n = 10)}$ = 7.1 %). The developed bio-strategy also exhibits high selectivity against potential interferents and a good stability of the nanotag for at least 2 months. Moreover, the developed method was successfully implemented to determine MPO in simulated chronic wound matrices, demonstrating its feasibility in a real scenario.

1. Introduction

Because of their prolonged healing process, frequently accentuated by factors such as aging, diabetes, obesity, or compromised immune response, among others, chronic wounds constitute a major health challenge [1–3]. These wounds are defined as those that do not heal in a short period of time, approximately less than 6 weeks, affecting to 1–2 % of the population in developed countries. This not only results in prolonged patient suffering but also places a significant burden on national healthcare systems, leading to escalated costs associated with extended hospital stays, an increased risk of secondary infections, and repeated medical action [4,5]. The patients' quality of life is totally affected, experiencing chronic pain, gradual loss of function and mobility which may even lead to an increased morbidity and mortality. A common example is the prevalence of diabetic foot ulcers, which frequently precede amputations [6], emphasizing the urgency of finding effective management strategies.

In contrast to conventional methods such as the non-specific analysis of clinical signs [7] and the evaluation of microorganisms, which may lack accuracy as indicators of infection [8], biomarkers are a swift and user-friendly alternative, allowing for a personalized treatment strategy based on individual profiles that facilitates the timely management of

* Corresponding author.
** Corresponding author at: NanoBioAnalysis Group-Department of Physical and Analytical Chemistry, University of Oviedo, Julián Clavería 8, Oviedo 33006, Spain.
E-mail addresses: susanacr@quim.ucm.es (S. Campuzano), alfredo.escosura@uniovi.es (A. de la Escosura-Muñiz).

https://doi.org/10.1016/j.snb.2025.137460
Received 11 October 2024; Received in revised form 13 January 2025; Accepted 15 February 2025
Available online 16 February 2025

treatment [9,10]. Different biomarkers, identified as potential detection targets of infection and healing monitoring status in chronic wounds, have been detected in wound exudate samples using biosensors. This is the case of hyaluronidase [11], lysozyme [12], sortase A and pyocyanin [13].

Among such biomarkers, myeloperoxidase (MPO) takes on a fundamental role as a protein expressed by neutrophilic leukocytes, essential contributors to host defence against infections [14]. Operating as a central mediator within the innate immune system, MPO is secreted to catalyse the formation of potent oxidizing molecules complexly involved in immune defence mechanisms against pathogens [15]. Consequently, MPO arises as a key biomarker for chronic wounds, owing to its significantly heightened activity in infected wounds compared to their non-infected counterparts, thereby it being quantified for diagnostic discernment [16,17]. Common methods for determining MPO include spectrophotometric [18] and fluorometric assays [19], cytological methods [20], and immunological techniques like ELISA [21] or Western blot [22]. Nevertheless, spectrophotometric assays may lack specificity [23], fluorometric assays may face issues with turbid samples [24], and immunological methods are usually tortuous and time-consuming [25] or lack quantification capability [26].

Electrochemical biosensors incorporating magnetic microsized beads (MBs) as bedrock represent a pivotal advancement in biomarker analysis, offering prominent advantages. These MBs-based bioplatforms substantially enhance sensitivity and kinetics of the assay, achieving exceptionally low limits of detection (LODs) for emerging biomarkers [27,28], and high selectivity, facilitating the accurate detection of specific biomarkers in complex sample matrices with minimal pretreatments and matrix effects [29]. Noteworthy, the attributes of these biosensors include their inherent convenience, cost-effectiveness, and point-of-care detection capabilities, thus playing a central role in elevating reliability in the realm of biomarker analysis [28]. Numerous biosensors employed for quantifying biomarkers, utilizing both optical and electrochemical methodologies, incorporate enzymatic labelling in their sensing mechanisms. Traditional enzyme markers, systems in which an immunoreactive agent is conjugated to one to four enzyme molecules [30], are widely used due to their simplicity, ease of fabrication, and straightforward kinetics. Interestingly, enzyme-loaded carriers can immobilize a higher number of enzyme molecules, which consequently enhances sensitivity, and lower LODs [31]. Additionally, carriers protect enzymes from interfering substances and harsh environmental conditions, ensuring better performance in complex environments and exhibiting greater thermal stability, increased pH tolerance, and extended shelf life [32], which leads to prolonged operational lifetime and highlight the superior performance of enzyme-loaded carriers compared to traditional single enzyme markers [33–35]. The most used enzyme carriers include gold nanoparticles [36], carbon nanotubes [37], various polymeric materials such as polystyrene beads and polyacrylamide [38], and inorganic materials like silica particles [39]. These carriers are favoured for their high surface area, biocompatibility, and ability to protect and stabilize enzymes, thereby enhancing the sensitivity and reliability of biosensors, but lacking the customizable porosity, extensive functionalization options, and structural tunability offered by Metal-Organic Frameworks (MOFs) [40].

MOFs, but particularly nanoMOFs, are emerging as promising alternatives for electrochemical labelling in biosensors due to their unique highly porous framework for accommodating biomolecules [41,42]. The inherent robustness of nanoMOFs under diverse environmental conditions [43,44], coupled with their biocompatibility [45], positions them as sturdy candidates for long-term and reliable biosensing applications. Additionally, the tuneable nature of nanoMOFs facilitates the design of multifunctional composite materials, allowing for the integration of multiple electroactive components to enhance detection capabilities [40]. Among its counterparts, the NH_2-MIL-101 (Fe) nanoMOF stands out for serving as a labelling entity in electrochemical biosensors due to both its exceptional functionality attributed to its amino groups [46], and the presence of iron in its structure, establishing an optimal synergistic effect particularly conducive to electrochemical detection [47]. However, the ability of this nanoMOF label to act as carrier of enzymatic tags in its porous structure, also protecting them from degradation, has not been exploited so far.

Acknowledging and benefiting from all these aspects, here we present an electrochemical immunosensor that takes advantage of and demonstrates for the first time the opportunities offered by the nanoMOF NH_2-MIL-101 (Fe) (hereinafter, nanoMOF) when loaded with the enzyme HRP, facilitating its function as a labelling agent. This configuration enables a higher HRP loading onto the nanoMOF than the conventional antibody-HRP conjugation, leading to increased sensitivity. Moreover, it addresses challenges associated with traditional enzymatic labelling methods, affording protection to the enzyme against adverse conditions [48], and enhancing stability during storage. There are several reasons why this specific nanoMOF is excellent for such application. First, the chemical synthesis is easy, leading to nanoparticles of around 260 nm with an acceptable polydispersity. Moreover, specific antibodies can be efficiently linked to the nanoMOF through the carbodiimide chemistry. Finally, the porous structure is ideal to accommodate and protect a high number of enzymatic tags.

This pioneering approach integrates the distinctive attributes of the nanoMOF decorated with both recognition and signaling biomolecules at will as a nanolabel with the inherent benefits of employing a sandwich-type immunoassay performed on MBs and utilizing screen-printed carbon electrodes (SPCEs) as transducers for MPO determination in chronic wounds, opening avenues for novel applications of these porous functional materials in electrochemical biosensing.

2. Materials and methods

Apparatus and electrodes, Reagents and solutions, and protocols followed for Synthesis of the nanoMOF, Preparation of DAb-nanoMOF (HRP), Structural characterization, Sandwich immunoassay on MBs, Amperometric transduction and Preparation and analysis of simulated chronic wound fluid are detailed in the Supporting Information.

3. Results and discussion

3.1. Synthesis and characterization of the nanoMOF

Fig. 1 schematically illustrates the steps involved in the synthesis (1a) and characterization (1b-d) of the nanoMOF. In summary, $FeCl_3{\cdot}6\ H_2O$ and aminoterephthalic acid underwent a 24-h reaction at 120 ºC to yield the nanoMOF, which was then rendered suitable for use through three successive washing steps via centrifugation, followed by a final vacuum drying overnight process.

Characterization of the synthetized nanoMOF by TEM showed rhomboidal-shape particles (Fig. 1b) whose size distribution histogram ($n = 214$), shown in Fig. 1c, gave an average mean diameter of (260 ± 40) nm with an acceptable polydispersity. Finally, the nanoMOF structure was confirmed by powder X-ray diffraction (PXRD) (Fig. 1d), agreeing well with results previously reported in the literature [49].

3.2. NanoMOF modification and characterization of the DAb-nanoMOF (HRP)

The synthetized nanoMOF was conjugated with DAb through carbodiimide chemistry taking advantage of the antibodies' carboxyl groups and the amino groups present in the structure of the nanoMOF for the formation of stable covalent bonds. At the same time, the HRP enzyme was encapsulated into the porous structure of the nanoMOF. An overview of the process is depicted in Fig. 2a.

The nanoMOF modification was characterized by amperometry, FTIR spectroscopy and ζ-potential measurements. Amperometric

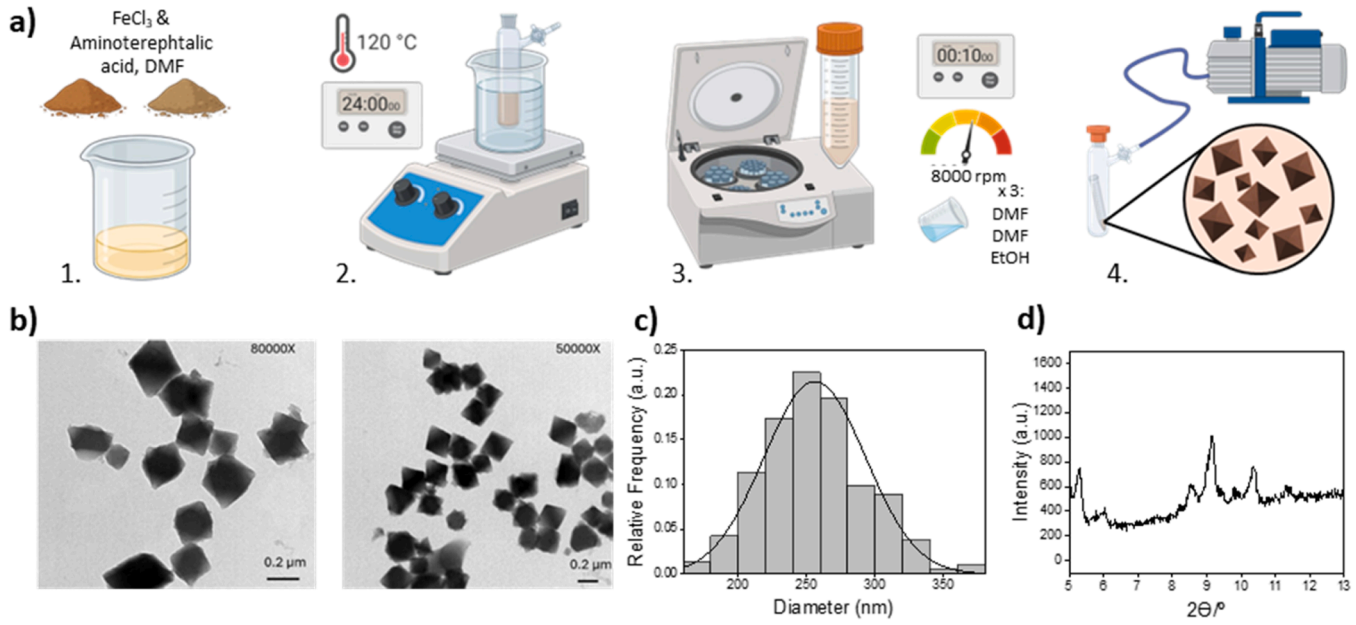

Fig. 1. Schematic diagram showing the steps involved in the preparation of the nanoMOF a) and its characterization. TEM images at 80000 × (b), left) and 50000 × (b), right), corresponding size distribution histogram c), and PXRD diagram d) are shown.

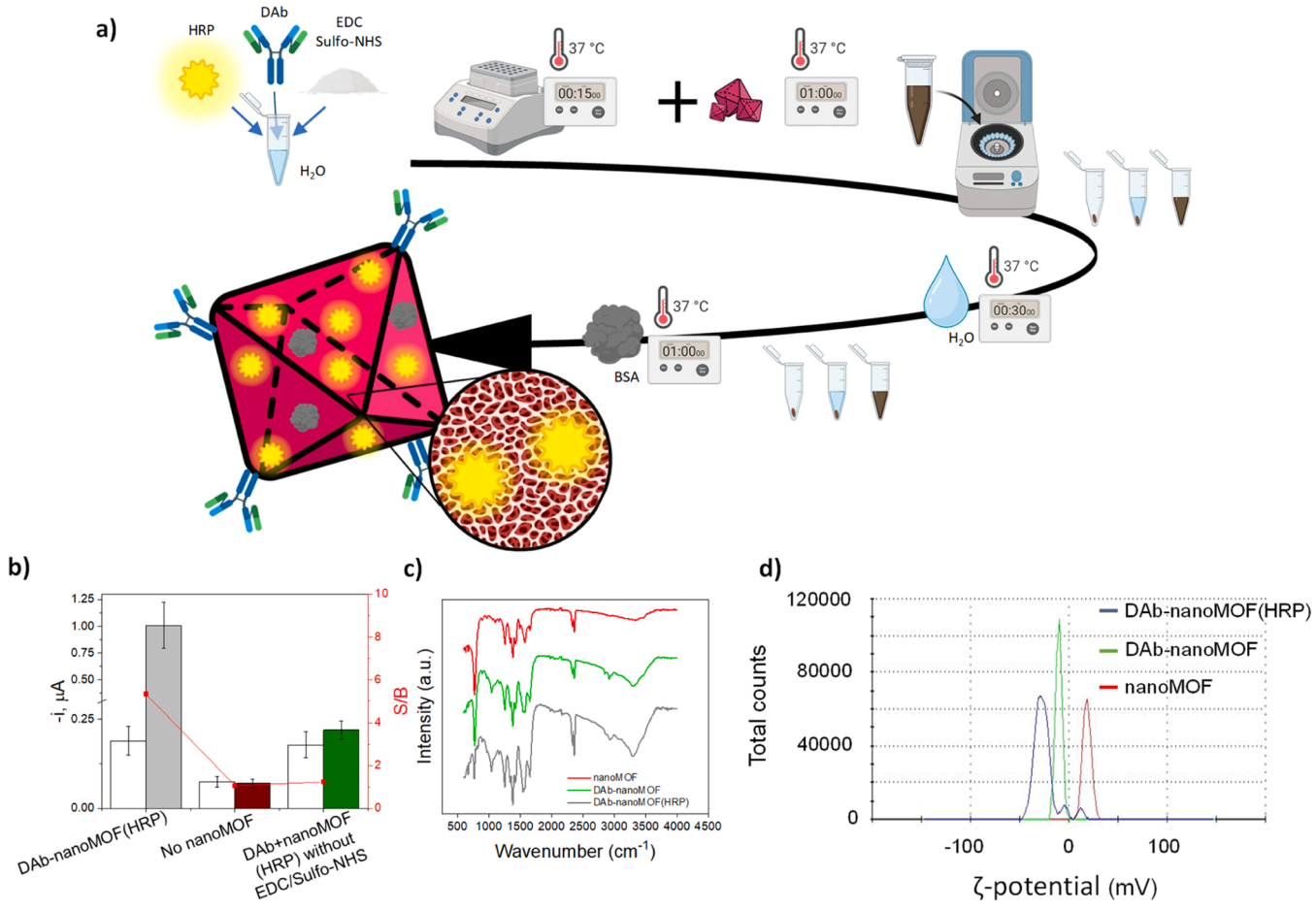

Fig. 2. Overview of the steps involved in the preparation of the DAb-nanoMOF(HRP) a), and its characterization by amperometry in the absence (white bars, B) and in the presence (colored bars, S) of 50 ng mL^{-1} MPO (B/S ratios are represented by red points connected by red lines) b), FTIR (nanoMOF (red trace); DAb-nanoMOF (green trace); DAb-nanoMOF(HRP) (grey trace) c), and ζ-potential measurements (nanoMOF (red trace); DAb-nanoMOF (green trace); DAb-nanoMOF-HRP (blue trace) d).

characterization (Fig. 2b) was performed following the same protocol than that used for MPO measurements. The obtained results revealed that the nanoMOF modification in the absence of the coupling agent (sulfo-NHS/EDC) (third column set of Fig. 2b) inhibited the nanoMOF functionalization with DAb and the generation of a significant signal in the presence of the target MPO. Moreover, the results obtained in the absence of nanoMOF clearly confirmed that the detected peroxidase activity was that of the HRP of the nanoMOF and not the intrinsic activity of the target (second column set of Fig. 2b). On the contrary, a substantial increase in the S/B ratio was reached when the nanoMOF was properly functionalized with DAb and HRP (first column set of Fig. 2b) thus verifying the possibility to carry out the detection of low MPO concentrations when using the appropriate biosensing design, as well as the covalent amide bond formation between the antibody and the nanoMOF.

The obtained FTIR spectra are shown in Fig. 2c, in which a spectrum of bare synthetized nanoMOF (red trace) is shown for comparative purposes to confirm the success of the conjugation. The comparison the bare nanoMOF spectrum with that of the DAb-nanoMOF(HRP) confirmed the conjugation process commented before. After DAb conjugation (green trace), an intensity increase in the 1650–1550 cm^{-1} region bands was observed, due to presence of amide groups of the proteins [50] as well as the appearance of a new band at around 1050 cm^{-1}, also attributable to the proteins [50], thus confirming the formation of covalent bonds between the nanoMOF structure and the antibody. The adsorption process of HRP (leading to its encapsulation into the porous structure of the nanoMOF) was confirmed by the broadening and increased intensity of the spectrum bands without any structural change (grey trace).

In addition, ζ-potential measurements were performed to study the conjugation process after both steps (covalent linking of DAb and adsorption of HRP), by evaluating the surface electrical potential of the nanoMOF. As shown in Fig. 2d, the synthetized nanoMOFs (red trace) showed a ζ-potential of (18 ± 4) mV, due to the presence of positive charges of the protonated amino groups in their structure. After DAb conjugation (green trace), a shift toward negative values ((−10 ± 3) mV) was observed, confirming the displacement of amino groups in the carbodiimide chemistry linking. Finally, the adsorption process of HRP onto the DAb modified NH_2-MIL101 (Fe) nanoMOF structure (blue trace) provoked a shift to still more negative values ((− 30 ± 10) mV). Therefore, the success of the conjugation process, as well as the good stability of the obtained conjugates, were confirmed by ζ-potential measurements.

3.3. Optimization of the key experimental parameters

As shown in Fig. 3a, the DAb-nanoMOF(HRP) served as nanocarrier of both recognition and signaling elements in a sandwich-type assay using Strep-MBs, with a biotinylated antibody as the capture recognition element (b-CAb). Moreover, the amperometric determination of MPO was accomplished by measuring the variation in the cathodic current in the presence of the H_2O_2/HQ redox system. In accordance with the assay

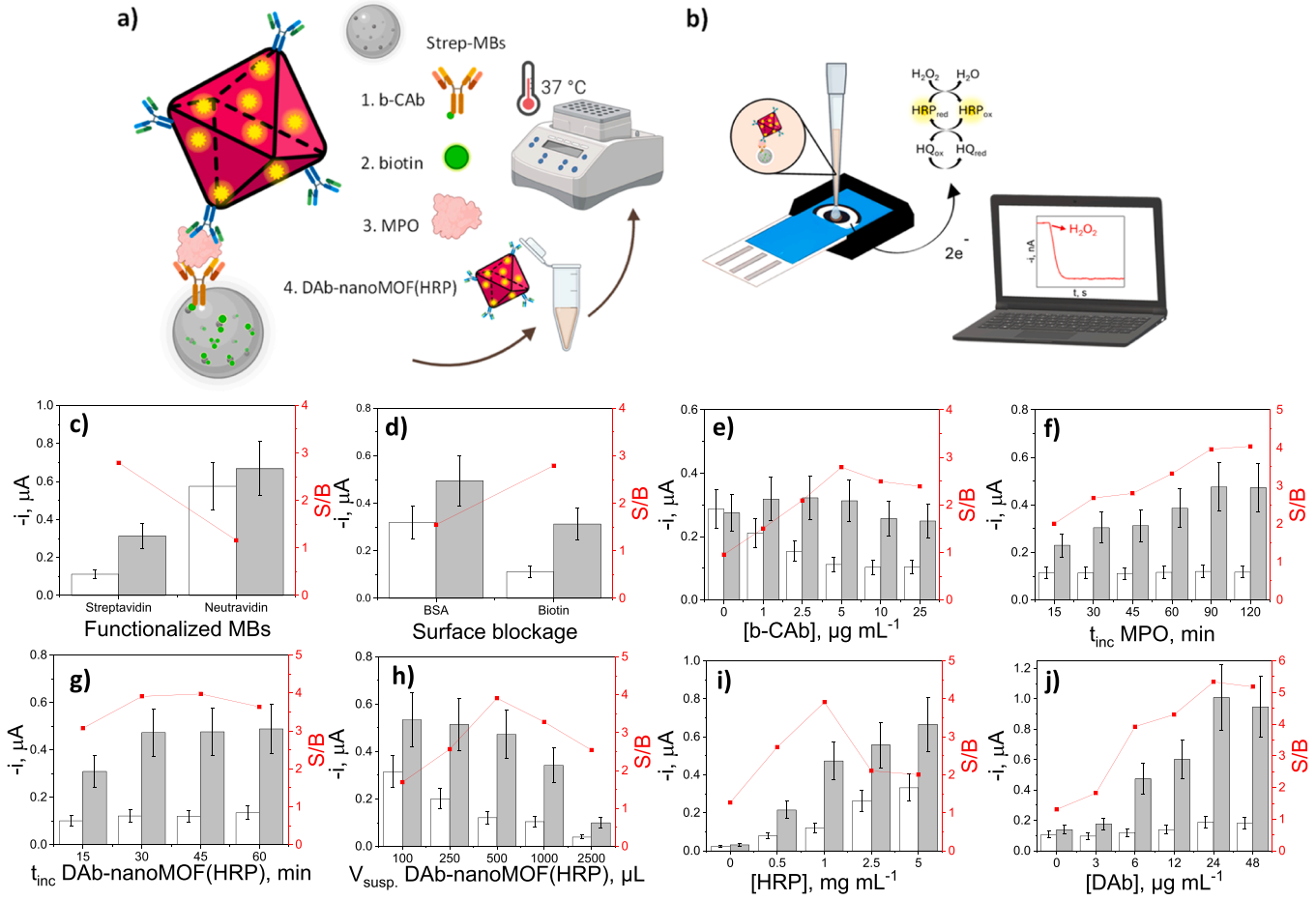

Fig. 3. Schematic diagram showing the steps involved in the preparation of the sandwich immunocomplexes on Strep-MBs a), and the amperometric transduction of the resulting magnetic bioconjugates at a SPCE b). Optimization of key experimental variables involved in the immunoplatform performance for MPO detection by comparing the amperometric readings obtained in the absence (white bars, B) and in the presence (grey bars, S) of 50 ng mL^{-1} MPO when varying functionalized MBs c), and their blockage d), b-CAb concentration e), incubation time of b-CAb-MBs with MPO standard solution f), DAb-nanoMOF(HRP) incubation time g) and concentration h), and HRP i) and DAb j) concentrations employed to functionalize the nanoMOF. The S/B ratios are represented as red squares connected by red lines.

configuration, such variation in the current was directly proportional to the MPO concentration (Fig. 3b).

The design of the immunosensor crafting was aimed at attaining point-of-care favorable features, employing a streamlined working protocol and minimizing assay duration. Therefore, the impact of key experimental variables on the biosensing response was carefully checked. Irrespective of the tested experimental variable, the selection criterion was based on the larger ratio between the currents measured by the immunoplatforms in the presence of 50 ng mL^{-1} MPO standards (S), and those without the target (B), respectively. The optimization studies, whose results are displayed in Fig. 3c-j, involved checking of bioassay variables such as the functionalization and blocking of the Strep-MBs, the concentration of the b-CAb, and the incubation times for MPO and DAb-nanoMOF(HRP), as well as variables related to the nanoMOF modification process including its resuspension volume and the concentration of HRP and DAb. Table 1 summarizes the evaluated ranges, along with the selected values.

As evidenced in Fig. 3c, Strep-MBs exhibited superior assay performance than Neu-MBs, the former producing much lower nonspecific adsorptions attributed to the DAb-nanoMOF(HRP) adhesion to the polymeric encapsulation layer of the beads, which differs depending on the manufacturer. The use of biotin as a blocking agent yielded a higher S/B ratio compared to BSA (Fig. 3d), probably owing to streptavidin's capacity to recognize multiple biotin molecules, potentially introducing steric hindrance to the adhesion of the modified nanoMOF onto the beads surface. Regarding the optimization of the b-CAb concentration, as shown in Fig. 3e, larger S/B ratio occurred for 5 μg mL^{-1}, which was used for further work. Furthermore, the measured blank values suggested that an increased antibody concentration decreased nonspecific adsorptions, which was confirmed by measuring the amperometric response when the b-CAb was substituted for a nonspecific biotinylated antibody (see Fig. S1 in the Supporting Information).

The measurements performed to determine the ideal incubation times for MPO and DAb-nanoMOF(HRP) are shown in Fig. 3f and g, revealing that better S/B ratios were found for 90 and 30 min, respectively, with no significant improvement for longer incubation periods. The volume where the nanoMOF was reconstituted after modification delineates its employed concentration, thus constituting a key variable to be considered. Fig. 3h shows that at small volumes, nonspecific adsorptions were higher, while large volumes hinder proper recognition and resulted in a substantial drop of the specific signal in the presence of MPO. Therefore, the same volume used for the entire modification process, 500 μL, was selected for further analysis. Furthermore, 1 mg mL^{-1} was chosen as the HRP concentration for loading the nanoMOF (Fig. 3i), as a compromise between increasing blanks and specific signals, both rising for higher enzyme concentrations, which led to smaller S/B ratios. It is important to note that the results shown in the "0" column set of Fig. 3i confirm both the correct functionalization of the nanoMOF with HRP and that the intrinsic peroxidase activity of the nanoMOF was not sufficient to discriminate the presence of the target protein. Finally, the selected DAb concentration for nanoMOF functionalization was 24 μg mL^{-1}, improving the efficacy of the immunoplatform and resulting in larger S/B ratio, which did not improve for a higher concentration, probably due to saturation of the nanoMOF anchoring sites with the DAb molecules (Fig. 3j). The significance of optimization assays in this work cannot be overstated, because it resulted in nearly a 100 % enhancement of the S/B ratio compared to the pre-optimization stage.

As evidenced by the concentration zero values, the deliberate exclusion of specific essential components from the immunoassay, such as b-CAb, DAb, or HRP ("0" set of bars in Fig. 3e, i and j) confirmed that the observed results, when none of them are lacking, are genuinely attributed to the intended interactions. Additionally, an unlabelled 50 ng mL^{-1} MPO concentration was tested to ascertain whether MPO itself could influence the electrochemical measurement due to its peroxidase activity. As can be seen in Fig. 2b, the outcome provided lower values than the blank, thus dismissing this possibility. This underscores the validity of the designed immunoassay, supporting the reliability and robustness of the experimental results.

Table 1
Summary of the optimized experimental parameters employed in the building of the MBs-assisted immunoplatform for the determination of MPO.

Parameter	Evaluated range	Selected value
Functionalized MBs	Strep-MBs, Neu-MBs	Streptavidin
Surface blockage	BSA or Biotin	Biotin
[b-CAb], μg mL^{-1}	0.0 – 25.0	5.0
MPO incubation time, min	15 – 120	90
DAb-nanoMOF(HRP) incubation time, min	15 – 60	30
DAb-nanoMOF(HRP) suspension volume, μL	100 – 2500	500
[HRP], mg mL^{-1}	0.0 – 5.0	1.0
[DAb], μg mL^{-1}	0.0 – 48.0	24.0

3.4. Analytical and operational characteristics

Under the optimized experimental conditions, the analytical features of the developed immunoplatform for the amperometric determination of MPO standards were established. In compliance with the utilized immunoassay format, the amperometric readings increased directly with the concentration of MPO, allowing the construction of the calibration plot depicted in Fig. 4 (black dots). A linear relationship between the amperometric measurements and the concentration of the target antigen was observed over the 5–100 ng mL^{-1} (r = 0.995) MPO concentration range, with slope and intercept values of (0.0172 ± 0.0006) μA mL ng^{-1} and (0.13 ± 0.03) μA, respectively.

Moreover, LOD and quantification (LOQ) values of 1.4 and 4.8 ng mL^{-1} were estimated using the 3 $\times s_b$/slope and 10 $\times s_b$/slope criteria, respectively, where s_b is the standard deviation of ten independent amperometric measurements made in the absence of MPO. The achieved sensitivity is adequate for MPO analysis, not only in chronic wound fluids, where it is highly overexpressed and does not pose a challenge for modern biosensors, but also in serum [51], plasma [52], or saliva [53] with considerably lower MPO concentrations at ng mL^{-1} level. This grants the immunosensing platform significant versatility,

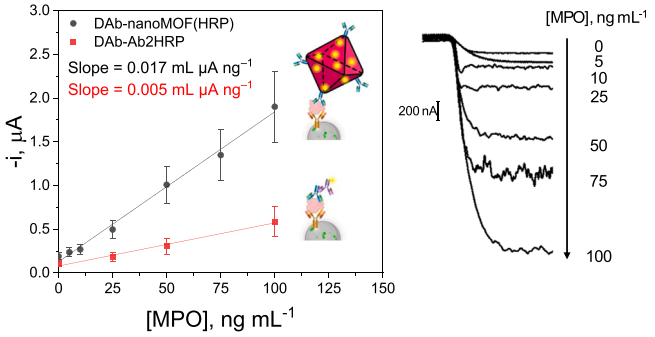

Fig. 4. Dependence of the amperometric response with the concentration of MPO standards prepared in buffered solution, obtained with the developed immunoplatform under the optimized working conditions -black dots- and its comparison with the method utilizing an HRP-tagged secondary antibody (Ab2HRP) as a label -red squares-. The methodology using Ab2HRP implied the same assay format but substituting the incubation step of the DAb-nanoMOF (HRP) for a combined incubation step with a mixture solution containing DAb (24 μg mL^{-1}) and Ab2HRP (2.5 μg mL^{-1}) in PBS for 30 min. Separate incubation of DAb and Ab2HRP and other incubation buffers (not shown) yielded poorer results. Actual amperograms recorded for the indicated MPO concentrations using the DAb-nanoMOF(HRP)-based immunoplatform are shown on the right in black.

given MPO's capacity to anticipate or contribute to the management of various diseases such as cancer [54], sepsis [55], lupus and cardiovascular diseases [56] or periodontitis [53].

Finally, a remarkable good reproducibility for the preparation of the immunoplatform is noteworthy, yielding a relative standard deviation (RSD) value for the measurements of 50 ng mL^{-1} MPO standard made with ten independently fabricated sensors of 7.1 %, thus highlighting the robustness and reliability of both the fabrication and detection processes.

3.5. Comparative labelling study

The comparative analysis of labelling strategies for the developed immunoplatform elucidated bold performance differences. The DAb-nanoMOF(HRP)-based approach involves a robust nanocarrier capable of accommodating a plethora of HRP molecules. Conversely, the sandwich method utilizing a secondary antibody tagged with a single HRP molecule (Ab2HRP), was tested. Calibration plots conducted with the immunoplatforms employing DAb-nanoMOF(HRP) and Ab2HRP as labelling modalities (Fig. 4), unequivocally underscore the marked superiority of the nanoMOF-based labelling approach, despite the other format appears to be also valid for MPO determination. This sensitivity-enhanced performance is attributed to the capability of the nanoMOF to accommodate a greater number of molecules, thereby substantiating its utility and preeminence in immunoassay methodologies.

Intending to check all possible configurations, other immunosensing formats were also tested. On one hand, given the reported intrinsic peroxidase activity of the nanoMOF [57], an attempt was made to implement the assay without HRP, seeking the ability of the nanoMOF itself to serve as electrochemical label. No discernment between the presence of 50 ng mL^{-1} MPO and its absence was achieved in this case, most likely because the attained sensitivity is not sufficient with this format. Moreover, to demonstrate the associated benefits of the peroxidase loading in the nanoMOF structure, the used label configuration (DAb-nanoMOF(HRP)) was compared with that involving substitution of the HRP loading by the HRP-labelled antibody (Ab2HRP) recognizing the DAb (Ab2HRP-DAb-nanoMOF). As it can be seen in Fig. S2 (in the Supporting Information) this format also failed, which can be attributed to either significantly lower sensitivity or potential failure of antibody recognition due to steric hindrance.

It should be mentioned that, recently, Ramos-López et al. have reported an immunoplatform for the determination of MPO that achieves similar detection and quantification limits in comparable assay times [58]. The authors use the same immunoreagents than us as well as MBs for the implementation of a sandwich immunoassay, while they employ cerium dioxide nanoparticles (CeO_2NPs)/multi-walled carbon nanotubes (MWCNTs) composites decorated with HRP-Strept as nanolabels. Besides the different nature of the nanolabels, the authors employed them solely as carriers of enzyme molecules (CeO_2/MWCNTs-(HRP--Strept)) and do not report their storage stability. Conversely, our developed immunoplatform uses the nanolabel also as a carrier of the detector antibody (DAb-nanoMOF(HRP)) and exhibiting a storage stability longer than 2 months (see next section). It is also important to highlight that, in the DAb-nanoMOF(HRP), the HRP molecules are encapsulated into the porous structure and not on the surface of the nanolabel, which makes it promising for application in denaturing media. Moreover, the role of the used antibodies is reversed (Ramos-López et al. used the biotinylated antibody as DAb while we use it as CAb), and the MBs are also different (HOOC-MBs or Strep-MBs). Taking all this into account, there are no important reasons to opt for one or the other nanolabel. Both of them can be envisaged as promising alternatives for further exploration.

3.6. Stability and selectivity

The stability and selectivity of the purposed system were evaluated. The DAb-nanoMOF(HRP) stability performance was truly striking, maintaining its S/B ratio unchanged for at least two months using sensors prepared on the same day (Fig. 5a). This feature can be attributed to the nanoMOF's framework capability to shield the HRP enzyme from adverse conditions [48], as well as to its capacity to accommodate many molecules within its pores. This remarkable stability is particularly interesting considering that the two described electrochemical sandwich immunoplatforms reported for the determination of MPO using other not-MOF nanolabels (AuNP@GMCHRP@Ab2 [59] and CeO_2NPs/MWCNTs-(HRP-Strept) [58]), did not report their stability over time.

In addition, the prepared b-CAb-MBs exhibited also a good storage stability, retaining functionality for over three weeks under refrigeration in filtered PBS, with consistent S/B ratios observed during control assessments as illustrated in Fig. S3 (in the Supporting Information). As can be observed, beyond day 21, nonspecific adsorptions increased notably. This may be due to the gradual detachment of antibodies from the MBs, which may have a comparable effect to that observed in Fig. S1, hindering the attachment of the modified nanoMOF to the MBs surface.

The presence of lysozyme and pyocyanin in wound fluids may potentially interfere with MPO detection. Lysozyme, an enzyme prevalent in bodily fluids and released by neutrophils, shares structural similarities with MPO [60,61], which may lead to cross-reactivity and false-positive responses. Moreover, pyocyanin, a phenazine pigment produced by a common wound pathogen, exhibits redox activity akin to MPO [62], which may complicate an accurate MPO detection. Therefore, the immunoplatform selectivity was evaluated by comparing the S/B ratios obtained for 0 and 50 ng mL^{-1} MPO in the absence and in presence of lysozyme and pyocyanin. The results are shown in Fig. 5b and confirmed that none of the scrutinized molecules identified as potential interferents caused a statistically significant disruption at the concentrations assayed (indicated in the figure caption).

It is important to mention at this point that the main objective of this work is to show a new applicability of a known nanoMOF modified *ad hoc* to demonstrate its advantages in sandwich immunosensing. For this purpose, MPO was selected as a model analyte, due to its recognized relevance as a marker of infection in wounds. Modification of the nanoMOF with HRP and DAb to function as a nanolabel in sandwich immunodetection led to an improved sensitivity (slope 3.4 times higher compared to conventional labelling using DAb/Ab2HRP, Fig. 4), and remarkable stability (at least 2 months).

If a comparison of the developed method with other reported for the determination of MPO is made, some conclusions arise. Commercial ELISA kits for MPO (ab119605 Myeloperoxidase Human ELISA Kit from Abcam; Human Myeloperoxidase DY3174 ELISA kit from R&D Systems) provide logarithmic calibration plots requiring longer determination times (4 h *vs.* 2 h, calculated from the CAb-coated ELISA plate and CAb-MBs), and instrumentation restricted to centralized environments (ELISA plate readers). Moreover, they have been developed for the determination of MPO in cell culture supernatant, serum and plasma, but not in wound exudates samples. With respect to the electrochemical immunosensors and immunoassays for MPO reported in the last decade (main features are summarized in Table S1 in the Supporting Information), although the limit of detection achieved with the developed immunoplatform is not as good as those claimed in the literature, the developed method still provides a detection ability of biomedical interest, as demonstrated by the results obtained in the analysis of wound exudate samples, a matrix not explored with any of the electrochemical immunosensing technologies described before.

3.7. Application to the analysis of simulated wound exudate samples

To demonstrate the applicability of the developed immunoplatform, samples of simulated wound fluids were prepared using two different processes, each representing scenarios of contrasting complexity.

The first scenario, illustrated in Fig. 6a, involved harsher conditions,

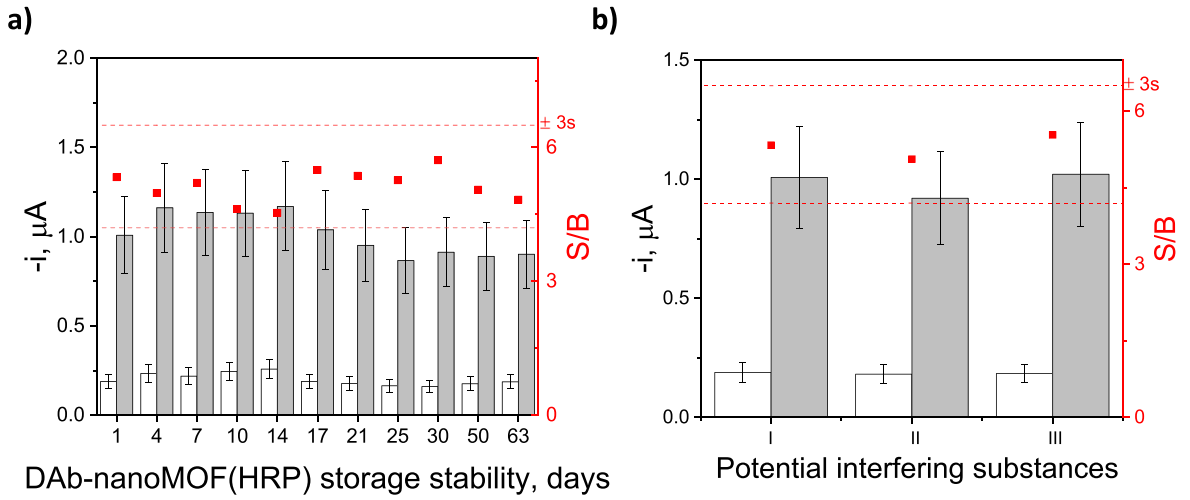

Fig. 5. a) Storage stability of DAb-nanoMOF(HRP). b) Selectivity of the proposed immunoplaform. Comparison of the amperometric responses measured in the absence of interference (I) and in the presence of 50 µg mL^{-1} lysozyme (II) and 100 ng mL^{-1} pyocyanin (III). S/B ratio values (red squares) provided for 0 (white bars) and 50 (grey bars) ng mL^{-1} MPO standards. Control limits were set at ± 3 s of the mean value provided by three immunoplatforms prepared in the first assay day a) or in the absence of interferents b).

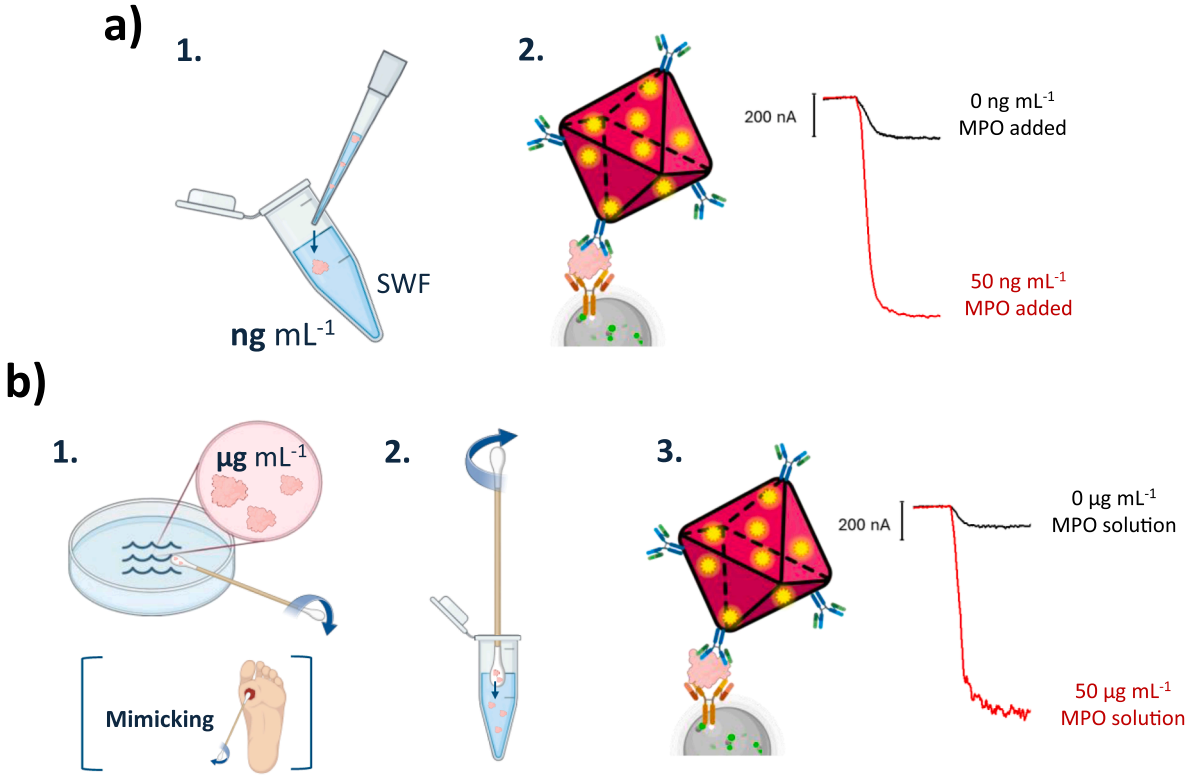

Fig. 6. Schematic representation of the two methods used to assess the applicability of the immunoplatform: MPO spiked at low concentrations in simulated wound fluids (SWFs) a), and replication of the Levine methodology b). The first approach involves the addition of small MPO concentrations to SWF a1), subsequently determined using the immunoplatform described in this work a2). The second method begins by soaking a swab in a MPO solution of high concentration, thus mimicking a chronic wound sample b1), followed by transferring its contents to PBS b2), and concluding with the determination process b3). Representative amperograms of samples analyzed by both methodologies are included in the Figure.

where two previously reported simulated matrices of chronic wounds (prepared as described in section "Preparation and analysis of simulated chronic wound fluid" in the Supporting Information) were spiked with low MPO concentrations (15, 25, and 50 ng mL^{-1}). The amperometric currents obtained for the first simulated medium (SWF1, containing NaCl, sodium bicarbonate ($NaHCO_3$), KCl, calcium chloride ($CaCl_2$) and BSA [63]) were interpolated into the calibration graph prepared with standard MPO solutions (Fig. 4), while the responses obtained for the second medium (SWF2, containing NaCl, $MgCl_2$, $CaCl_2$, $CaCO_3$, glucose, BSA, and lactic acid [64]), were interpolated into a calibration graph constructed in the SWF2 matrix itself, due to the slightly slower amperometric signals obtained for the standards prepared in this matrix compared to those prepared in buffer (see Fig. S4 in the Supporting Information). These results were attributed to the high BSA

concentration in SWF2 (5 % *vs.* 3 % BSA in SWF1), a well-known blocking agent [65] which has previously been observed that can partially block the surface of the MBs [66].

The second scenario, schematized in Fig. 6b, tried to replicate more realistic clinical conditions by mimicking Levine's swab wound sampling technique. The swab was rotated in a highly concentrated MPO solution emulating the content of infected and non-infected wounds (11, 50 and 100 μg mL^{-1} [16,67]). The MPO absorbed by the swab was subsequently transferred to PBS to perform the determination.

The obtained results by applying the two methodologies (Tables 2 and 3, respectively) were satisfactory, with recoveries close to 100 %, in all cases thus proving the feasibility of the developed immunoplatform to determine MPO in a real scenario.

4. Conclusions

In this work we have taken advantage, for the first time, of the porous and functional structure of the NH_2-MIL-101 (Fe) nanoMOF, for its use as advantageous enzyme-carrier nanotag in immunoassays. The tagging method harnesses the unique properties of the nanoMOF, relying on the covalent attachment of specific MPO detection antibodies onto the surface of the framework and the use of adsorbed HRP molecules as enzymatic tags. The porous structure of the nanoMOF allows using a large HRP loading as well as its protection from degradation inside the pores providing a high stability. This together with the ability of the nanoMOF to link antibodies through its functional groups makes the nanotag a very robust and powerful label.

This innovative approach significantly enhances the analytical characteristics of conventional sandwich immunoassay formats, achieving more than a threefold improvement in sensitivity. The use of nanoMOFs in this context not only exploits their inherent structural and functional benefits but also introduces a new dimension of stability to the tagging process, ensuring more reliable and reproducible results and highlighting its capacity to tackle greater challenges within the field of electrochemical biosensing. Furthermore, we have successfully pioneered an immunosensing platform for MPO determination that showcases remarkable potential for seamless integration into clinical practice. The excellent analytical characteristics reached (LOD of 1.4 ng mL^{-1} and operational dynamic range from 5–100 ng mL^{-1}) allowed its applicability to the accurate analysis of MPO in simulated chronic wound fluids yielding recovery percentages close to 100 %, underscoring its potential applicability for the detection and monitoring of MPO in clinical settings. The developed method can be envisaged as a relevant contribution to the application of robust nanoMOFs in electrochemical tagging and immunosensing, offering a powerful tool for advancing both research and versatile clinical practices in the field of biosensing and diagnostics (not only electrochemical). It is also important to highlight that the protection of the HRP encapsulated in the porous structure of the nanoMOF could be used for immunosensing of this or other targets in other matrices with denaturing components or pH values such as gastric mucosa. Overall, we envisage a universal use of this innovative label that may be extended for any other immunoassay, targeting applications in medicine, food analysis and environmental control among other fields.

CRediT authorship contribution statement

Campuzano Susana: Writing – review & editing, Writing – original draft, Supervision, Resources, Funding acquisition, Conceptualization. **de la Escosura-Muñiz Alfredo:** Writing – review & editing, Writing – original draft, Supervision, Resources, Funding acquisition, Conceptualization. **García-Alonso Francisco J.:** Writing – review & editing, Writing – original draft, Supervision, Resources, Funding acquisition, Conceptualization. **Pingarrón José M.:** Writing – review & editing, Resources. **Torrente-Rodríguez Rebeca M.:** Writing – review & editing, Writing – original draft, Supervision. **Pedrero María:** Writing – review & editing, Writing – original draft, Supervision. **Pérez-Ginés Víctor:** Writing – review & editing, Writing – original draft, Methodology, Investigation. **Valero-Calvo David:** Writing – review & editing, Writing – original draft, Methodology, Investigation.

Table 2
Results provided by the immunoplatform in the analysis of spiked simulated wound fluids (SWFs) using the protocol depicted in Fig. 6a.

	$[MPO]_{added}$, ng mL^{-1}	$[MPO]_{found}$, ng mL^{-1}	Recovery, %
SWF1	10	9.5 ± 0.6	95 ± 6
	25	24 ± 1	98 ± 5
	50	50 ± 3	100 ± 7
SWF2	10	9.9 ± 0.9	99 ± 9
	25	26 ± 1	103 ± 6
	50	47 ± 4	95 ± 8

Table 3
Results provided by the immunoplatform mimicking Levine's swab-based sampling method using the protocol depicted in Fig. 6b.

$[MPO]_{added}$, μg mL^{-1}	$[MPO]_{found}$, μg mL^{-1}	Recovery, %
11	10.2 ± 0.9	92 ± 9
50	47 ± 3	95 ± 6
100	100 ± 7	100 ± 7

Declaration of Competing Interest

The authors declare that they have no known competing financial interests or personal relationships that could have appeared to influence the work reported in this paper.

Acknowledgements

The financial support of Grants PID2020-115204RB-I00, RED2022-134120-T and PID2022-136351OB-I00, funded by MCIN/AEI/10.13039/501100011033 and by "ERDF A way of making Europe" and SV-PA-21-AYUD/2021/51323 from the Asturias Regional Government is gratefully acknowledged. V.P.G. acknowledges a predoctoral contract from Complutense University of Madrid and D.V.C. acknowledges a predoctoral FPI Grant from the MCIN (PRE2021–097567).

Appendix A. Supporting information

Supplementary data associated with this article can be found in the online version at doi:10.1016/j.snb.2025.137460.

Data availability

Data will be made available on request.

References

[1] F.A.R. Mota, S.A.P. Pereira, A.R.T.S. Araújo, M.L.C. Passos, M.L.M.F.S. Saraiva, Biomarkers in the diagnosis of wounds infection: an analytical perspective, TrAC, Trends Anal. Chem. 143 (2021) 116405, https://doi.org/10.1016/j.trac.2021.116405.
[2] R.J.R.S. Thanapaul, M. Shvedova, G.H. Shin, D.S. Roh, An insight into aging, senescence, and their impacts on wound healing, Adv. Geriatr. Med. Res. 3 (3) (2021) e210017, https://doi.org/10.20900/agmr20210017.
[3] A. Alma, G.D. Marconi, E. Rossi, C. Magnoni, A. Paganelli, Obesity and wound healing: focus on mesenchymal stem cells, Life 13 (3) (2023) 717, https://doi.org/10.3390/life13030717.
[4] K. Järbrink, G. Ni, H. Sönnergren, A. Schmidtchen, C. Pang, R. Bajpai, J. Car, The humanistic and economic burden of chronic wounds: a protocol for a systematic review, Syst. Rev. 6 (2017) 15, https://doi.org/10.1186/s13643-016-0400-8.
[5] C.K. Sen, Human wound and its burden: updated 2020 compendium of estimates, Adv. Wound Care 10 (5) (2021) 281–292, https://doi.org/10.1089/wound.2021.0026.
[6] R.C. Chamberlain, K. Fleetwood, S.H. Wild, H.M. Colhoun, R.S. Lindsay, J. R. Petrie, R.J. McCrimmon, F. Gibb, S. Philip, N. Sattar, B. Kennon, G.P. Leese, Foot

ulcer and risk of lower limb amputation or death in people with diabetes: a national population-based retrospective cohort study, Diabetes Care 45 (1) (2022) 83–91, https://doi.org/10.2337/dc21-1596.
[7] M. Reddy, S.S. Gill, W. Wu, S.R. Kalkar, P.A. Rochon, Does this patient have an infection of a chronic wound? JAMA, J. Am. Med. Assoc. 307 (6) (2012) 605–611, https://doi.org/10.1001/jama.2012.98.
[8] D.T. Williams, J.R. Hilton, K.G. Harding, Diagnosing foot infection in diabetes, Clin. Infect. Dis. 39 (2) (2004) S83–S88, https://doi.org/10.1086/383267.
[9] M.A. Weigelt, H.A. Lev-Tov, M. Tomic-Canic, W.D. Lee, R. Williams, D. Strasfeld, R. S. Kirsner, I.M. Herman, Advanced wound diagnostics: toward transforming wound care into precision medicine, Adv. Wound Care 11 (6) (2022) 330–359, https://doi.org/10.1089/wound.2020.1319.
[10] C. Yang, C. Yang, Y. Chen, J. Liu, Z. Liu, H.J. Chen, The trends in wound management: sensing, therapeutic treatment, and "theranostics, J. Sci.: Adv. Mater. Devices 8 (4) (2023) 100619, https://doi.org/10.1016/j.jsamd.2023.100619.
[11] C. Toyos-Rodríguez, A. Adawy, F.J. García-Alonso, A. de la Escosura-Muñiz, Enhancing the electrocatalytic activity of palladium nanocluster tags by selective introduction of gold atoms: application for a wound infection biomarker detection, Biosens. Bioelectron. 200 (2022) 113926, https://doi.org/10.1016/j.bios.2021.113926.
[12] A. Iglesias-Mayor, O. Amor-Gutiérrez, C. Toyos-Rodríguez, A. Bassegoda, T. Tzanov, A. de la Escosura-Muñiz, Electrical monitoring of infection biomarkers in chronic wounds using nanochannels, Biosens. Bioelectron. 209 (2022) 114243, https://doi.org/10.1016/j.bios.2022.114243.
[13] Z. Shi, C. Dai, P. Deng, X. Li, Y. Wu, J. Lv, C. Xiong, Y. Shuai, F. Zhang, D. Wang, H. Liang, Y. He, Q. Chen, Y. Lu, Q. Liu, Wearable battery-free smart bandage with peptide functionalized biosensors based on MXene for bacterial wound infection detection, Sens. Actuators B: Chem. 383 (2023) 133598, https://doi.org/10.1016/j.snb.2023.133598.
[14] Y. Aratani, Myeloperoxidase: its role for host defense, inflammation, and neutrophil function, Arch. Biochem. Biophys. 640 (2018) 47–52, https://doi.org/10.1016/j.abb.2018.01.004.
[15] M.J. Davies, C.L. Hawkins, The role of myeloperoxidase in biomolecule modification, chronic inflammation, and disease, Antioxid. Redox Signal. 32 (13) (2020) 957–981, https://doi.org/10.1089/ars.2020.8030.
[16] A. Hasmann, E. Wehrschuetz-Sigl, A. Marold, H. Wiesbauer, R. Schoeftner, U. Gewessler, A. Kandelbauer, D. Schiffer, K.P. Schneider, B. Binder, M. Schintler, G.M. Guebitz, Analysis of myeloperoxidase activity in wound fluids as a marker of infection, Ann. Clin. Biochem. 50 (3) (2013) 245–254, https://doi.org/10.1258/acb.2011.010249.
[17] A. Bassegoda, G. Ferreres, S. Pérez-Rafael, D. Hinojosa-Caballero, J. Torrent-Burgués, T. Tzanov, New myeloperoxidase detection system based on enzyme-catalysed oxidative synthesis of a dye for paper-based diagnostic devices, Talanta 194 (2019) 469–474, https://doi.org/10.1016/j.talanta.2018.10.065.
[18] Y. Xia, J.L. Zweier, Measurement of myeloperoxidase in leukocyte-containing tissues, Anal. Biochem. 245 (1) (1997) 93–96, https://doi.org/10.1006/abio.1996.9940.
[19] R. Majid, Z.A. Al Talebi, H.S. Al-Kawaz, A.H. Alta'ee, A.R.S. Alsalman, A. M. Hadwan, M.M. Hadwan, M.H. Hadwan, Novel fluorometric protocol for assessing myeloperoxidase activity, Enzym. Microb. Technol. 171 (2023) 110320, https://doi.org/10.1016/j.enzmictec.2023.110320.
[20] M. Kitahara, Y. Simonian, H.J. Eyre, Neutrophil myeloperoxidase: a simple, reproducible technique to determine activity, J. Lab. Clin. Med. 93 (2) (1979) 232–237. PMID 219116.
[21] S. Wakasugi-Onogi, S. Ma, R.T. Ruhee, Y. Tong, Y. Seki, K. Suzuki, Sulforaphane attenuates neutrophil ROS production, MPO degranulation and phagocytosis, but does not affect NET formation *ex vivo* and *in vitro*, Int. J. Mol. Sci. 24 (2023) 8479, https://doi.org/10.3390/ijms24108479.
[22] Y. Sawayama, Y. Miyazaki, K. Ando, K. Horio, C. Tsutsumi, D. Imanishi, H. Tsushima, Y. Imaizumi, T. Hata, T. Fukushima, S. Yoshida, Y. Onimaru, M. Iwanaga, J. Taguchi, K. Kuriyama, M. Tomonaga, Expression of myeloperoxidase enhances the chemosensitivity of leukemia cells through the generation of reactive oxygen species and the nitration of protein, Leukemia 22 (2008) 956–964, https://doi.org/10.1038/leu.2008.8.
[23] O. Mozgova, M. Blazheyevskiy, L. Kryskiw, T. Kucher, O. Shliusar, V. Moroz, Determination of prothipendyl by difference spectrophotometric method based on the absorption of its sulfoxide, Chem. Pap. 78 (2024) 2613–2619, https://doi.org/10.1007/s11696-023-03266-5.
[24] D. Rajnovic, J. Mas, Fluorometric detection of phages in liquid media: application to turbid simples, Anal. Chim. Acta 1111 (2020) 23–30, https://doi.org/10.1016/j.aca.2020.03.016.
[25] A. Onopiuk, A. Tokarzewicz, E. Gorodkiewicz, Cystatin C: a kidney function biomarker, Adv. Clin. Chem. 68 (2015) 57–69, https://doi.org/10.1016/bs.acc.2014.11.007.
[26] T. Mahmood, P.C. Yang, Western blot: technique, theory, and trouble shooting, N. Am. J. Med. Sci. 4 (9) (2012) 429–434, https://doi.org/10.4103/1947-2714.100998.
[27] Á. Molinero-Fernández, M. Moreno-Guzmán, M.Á. López, A. Escarpa, Magnetic bead-based electrochemical immunoassays on-drop and on-chip for procalcitonin determination: disposable tools for clinical sepsis diagnosis, Biosensors 10 (6) (2020) 66, https://doi.org/10.3390/bios10060066.
[28] Y. Chang, Y. Wang, J. Zhang, Y. Xing, G. Li, D. Deng, L. Liu, Overview on the design of magnetically assisted electrochemical biosensors, Biosensors 12 (11) (2022) 954, https://doi.org/10.3390/bios12110954.
[29] S. Fortunati, M. Giannetto, C. Giliberti, M. Mattarozzi, A. Bertucci, M. Careri, Magnetic beads as versatile tools for electrochemical biosensing platforms in point-of-care testing, Anal. Sens. 4 (3) (2023) e202300062, https://doi.org/10.1002/anse.202300062.
[30] S. Regidi, S. Ravindran, A.L. Vijayan, V. Maya, L. Sreedharan, J. Varghese, K. Ramaswami, M. Gopi, Effect of lyophilization on HRP–antibody conjugation: an enhanced antibody labeling technology, BMC Res. Notes 11 (2018) 596, https://doi.org/10.1186/s13104-018-3688-8.
[31] N.M. Kilic, S. Singh, G. Keles, S. Cinti, S. Kurbanoglu, D. Odaci, Novel approaches to enzyme-based electrochemical nanobiosensors, Biosensors 13 (6) (2023) 622, https://doi.org/10.3390/bios13060622.
[32] M. Spasojević, O. Prodanović, N. Pantić, N. Popović, A.M. Balaž, R. Prodanović, The enzyme immobilization: carriers and immobilization methods, J. Eng. Process. Manag. 11 (2) (2019) 89–105, https://doi.org/10.7251/JEPM1902089S.
[33] A. Koyappayil, M.H. Lee, Ultrasensitive materials for electrochemical biosensor labels, Sensors 21 (1) (2021) 89, https://doi.org/10.3390/s21010089.
[34] H.K. Choi, J. Yoon, Enzymatic electrochemical/fluorescent nanobiosensor for detection of small chemicals, Biosensors 13 (4) (2023) 492, https://doi.org/10.3390/bios13040492.
[35] D.M. Liu, C. Dong, Recent advances in nano-carrier immobilized enzymes and their applications, Process Biochem 92 (2020) 464–475, https://doi.org/10.1016/j.procbio.2020.02.005.
[36] Y. Cao, L. Wen, F. Svec, T. Tan, Y. Lv, Magnetic AuNP@Fe3O4 nanoparticles as reusable carriers for reversible enzyme immobilization, Chem. Eng. J. 286 (2016) 272–281, https://doi.org/10.1016/j.cej.2015.10.075.
[37] P. Fan, L. Liu, Q. Guo, J. Wang, J. Yang, X. Guan, S. Chen, H. Hou, Three-dimensional N-doped carbon nanotube@carbon foam hybrid: an effective carrier of enzymes for glucose biosensors, RSC Adv. 7 (2017) 26574, https://doi.org/10.1039/C7RA02592K.
[38] J.M. González-Sáiz, C. Pizarro, Polyacrylamide gels as support for enzyme immobilization by entrapment. Effect of polyelectrolyte carrier, pH and temperature on enzyme action and kinetics parameters, Eur. Polym. J. 37 (3) (2001) 435–444, https://doi.org/10.1016/S0014-3057(00)00151-8.
[39] L. Zhao, Y. Zhang, Y. Yang, C. Yu, Silica-based nanoparticles for enzyme immobilization and delivery, Chem. - Asian J. 17 (17) (2022) e202200573, https://doi.org/10.1002/asia.202200573.
[40] A.E. Baumann, D.A. Burns, B. Liu, V.S. Thoi, Metal-organic framework functionalization and design strategies for advanced electrochemical energy storage devices, Commun. Chem. 2 (2019) 86, https://doi.org/10.1038/s42004-019-0184-6.
[41] J.E. da, S. Souza, G.P. de Oliveira, J.Y.N.H. Alexandre, J.G.L. Neto, M.B. Sales, P.G. de S. Junior, A.L.B. de Oliveira, M.C.M. de Souza, J.C.S. dos Santos, A comprehensive review on the use of metal–organic frameworks (MOFs) coupled with enzymes as biosensors, Electrochem 3 (1) (2022) 89–113, https://doi.org/10.3390/electrochem3010006.
[42] M. Li, G. Zhang, A. Boakye, H. Chai, L. Qu, X. Zhang, Recent advances in metal-organic framework-based electrochemical biosensing applications, Front. Bioeng. Biotechnol. 9 (2021) 797067, https://doi.org/10.3389/fbioe.2021.797067.
[43] Z. Wang, A. Bilegsaikhan, R.T. Jerozal, T.A. Pitt, P.J. Milner, Evaluating the robustness of metal–organic frameworks for synthetic chemistry, ACS Appl. Mater. Interfaces 13 (15) (2021) 17517–17531, https://doi.org/10.1021/acsami.1c01329.
[44] M. Al-Shaeli, S.J.D. Smith, S. Jiang, H. Wang, K. Zhang, B.P. Ladewig, Long-term stable metal organic framework (MOF) based mixed matrix membranes for ultrafiltration, J. Membr. Sci. 635 (2021) 119339, https://doi.org/10.1016/j.memsci.2021.119339.
[45] S. Zhang, F. Rong, C. Guo, F. Duan, L. He, M. Wang, Z. Zhang, M. Kang, M. Du, Metal–organic frameworks (MOFs) based electrochemical biosensors for early cancer diagnosis *in vitro*, Coord. Chem. Rev. 439 (2021) 213948, https://doi.org/10.1016/j.ccr.2021.213948.
[46] P. Karthik, A. Pandikumar, M. Preeyanghaa, M. Kowsalya, B. Neppolian, Amino-functionalized MIL-101(Fe) metal-organic framework as a viable fluorescent probe for nitroaromatic compounds, 2265−22, Microchim. Acta 184 (2017), https://doi.org/10.1007/s00604-017-2215-2.
[47] X. He, Fundamental perspectives on the electrochemical water applications of metal–organic frameworks, Nano-Micro Lett. 15 (2023) 148, https://doi.org/10.1007/s40820-023-01124-3.
[48] J. Qiao, C. Cheng, D. Li, L. Qi, Thermo-responsive polymer-modified metal–organic frameworks as soft–rigid enzyme-reactors for enhancement of enzymolysis efficiency using a controllable embedding protocol, J. Mater. Chem. B 11 (2023) 6428–6434, https://doi.org/10.1039/D3TB00844D.
[49] Z. Zhang, X. Li, B. Liu, Q. Zhao, G. Chen, Hexagonal microspindle of NH_2-MIL-101 (Fe) metal–organic frameworks with visible-light-induced photocatalytic activity for the degradation of toluene, RSC Adv. 6 (2016) 4289–4295, https://doi.org/10.1039/C5RA23154J.
[50] A. Barth, Infrared spectroscopy of proteins, Biochim. Biophys. Acta 1767 (2007) 1073–1101, https://doi.org/10.1016/j.bbabio.2007.06.004.
[51] N. Vaguliene, M. Zemaitis, S. Lavinskiene, S. Miliauskas, R. Sakalauskas, Local and systemic neutrophilic inflammation in patients with lung cancer and chronic obstructive pulmonary disease, BMC Immunol. 14 (2013) 36, https://doi.org/10.1186/1471-2172-14-36.
[52] B. Pastor, J.D. Abraham, E. Pisareva, C. Sanchez, A. Kudriavstev, R. Tanos, A. Mirandola, L. Mihalovičová, V. Pezzella, A. Adenis, M. Ychou, T. Mazard, A. R. Thierry, Association of neutrophil extracellular traps with the production of circulating DNA in patients with colorectal cancer, iScience 25 (2022) 103826, https://doi.org/10.1016/j.isci.2022.103826.
[53] I. Carrillo-Novia, Estatus antioxidante e inmunitario salival en adultos con periodontitis crónica, Tesis de Licenciatura, Universidad Autónoma del Estado de

México, http://hdl.handle.net/20.500.11799/65265, 2014 (accessed 9 October 2024).
[54] M. Weng, Y. Yue, D. Wu, C. Zhou, M. Guo, C. Sun, Q. Liao, M. Sun, D. Zhou, C. Miao, Increased MPO in colorectal cancer is associated with high peripheral neutrophil counts and a poor prognosis: a TCGA with propensity score-matched analysis, Front. Oncol. 12 (2022) 940706, https://doi.org/10.3389/fonc.2022.940706.
[55] A. Bonaventura, F. Carbone, A. Vecchié, J. Meessen, S. Ferraris, E. Beck, R. Keim, S. Minetti, E. Elia, D. Ferrara, A.M. Ansaldo, D. Novelli, P. Caironi, R. Latini, F. Montecucco, The role of resistin and myeloperoxidase in severe sepsis and septic shock: results from the ALBIOS trial, Eur. J. Clin. Invest. 50 (2020) e13333, https://doi.org/10.1111/eci.13333.
[56] M. Urquizu-Padilla, Actividad del lupus eritematoso sistémico y marcadores sanguíneos asociados a aterosclerosis, Tesis Doctoral, Universitat Autónoma de Barcelona, ⟨https://tesisenred.net/bitstream/handle/10803/4511/mup1de1.pdf?sequence= 1⟩, 2007 (accessed 9 October 2024).
[57] L. Li, D. Chen, B. Li, D. Yang, J. Zhao, D. Ma, L. Jiang, Y. Yang, Y. Li, J. Wang, MOFzyme: enzyme mimics of Fe/Fe-MIL-101, J. Biosci. Med. 7 (5) (2019) 213–221, https://doi.org/10.4236/jbm.2019.75023.
[58] C. Ramos-López, L. García-Rodrigo, E. Sánchez-Tirado, L. Agüí, A. González-Cortés, P. Yáñez-Sedeño, J.M. Pingarrón, Cerium dioxide-based nanostructures as signal nanolabels for current detection in the immunosensing determination of salivary myeloperoxidase, Microchem. J. 201 (2024) 110505, https://doi.org/10.1016/j.microc.2024.110505.
[59] B. Liu, L. Lu, Amperometric sandwich immunoassay for determination of myeloperoxidase by using gold nanoparticles encapsulated in graphitized mesoporous carbon, Microchim. Acta 186 (2019) 262, https://doi.org/10.1007/s00604-019-3359-z.
[60] I. Grishkovskaya, M. Paumann-Page, R. Tscheliessnig, J. Stampler, S. Hofbauer, M. Soudi, B. Sevcnikar, C. Oostenbrink, P.G. Furtmüller, K. Djinović-Carugo, W. M. Nauseef, C. Obinger, Structure of human promyeloperoxidase (proMPO) and therole of the propeptide in processing and maturation, J. Biol. Chem. 292 (20) (2017) 8244–8261, https://doi.org/10.1074/jbc.M117.775031.
[61] A.C. Gálvez-Iriqui, M. Plascencia-Jatomea, S. Bautista-Banos, Lysozymes: characteristics, mechanism of action and technological applications on the control of pathogenic microorganisms, Mex. J. Phytopathol. 38 (3) (2020) 360–383, https://doi.org/10.18781/r.mex.fit.2005-6.
[62] H. Shouman, H.S. Said, H.I. Kenawy, R. Hassan, Molecular and biological characterization of pyocyanin from clinical and environmental *Pseudomonas aeruginosa*, Microb. Cell Fact. 22 (2023) 166, https://doi.org/10.1186/s12934-023-02169-0.
[63] E.S. Sani, C. Xu, C. Wang, Y. Song, J. Min, J. Tu, S.A. Solomon, J. Li, J.L. Banks, D. G. Armstrong, W. Gao, A stretchable wireless wearable bioelectronic system for multiplexed monitoring and combination treatment of infected chronic wounds, Sci. Adv. 9 (12) (2023) eadf7388, https://doi.org/10.1126/sciadv.adf7388.
[64] M. Galliani, C. Diacci, M. Berto, M. Sensi, V. Beni, M. Berggren, M. Borsari, D. T. Simon, F. Biscarini, C.A. Bortolotti, Flexible printed organic electrochemical transistors for the detection of uric acid in artificial wound exudate, Adv. Mater. Interfaces 7 (23) (2020) 2001218, https://doi.org/10.1002/admi.202001218.
[65] D. Huber, J. Rudolf, P. Ansari, B. Galler, M. Führer, C. Hasenhindl, S. Baumgartner, Effectiveness of natural and synthetic blocking reagents and their application for detecting food allergens in enzyme-linked immunosorbent assays, Anal. Bioanal. Chem. 394 (2009) 539–548, https://doi.org/10.1007/s00216-009-2698-8.
[66] V. Ruiz-Valdepeñas Montiel, S. Campuzano, F. Conzuelo, R.M. Torrente-Rodríguez, M. Gamella, A.J. Reviejo, J.M. Pingarrón, Electrochemical magnetoimmunosensing platform for determination of the milk allergen β-lactoglobulin, Talanta 131 (2015) 156–162, https://doi.org/10.1016/j.talanta.2014.07.076.
[67] J. Hoyo, A. Bassegoda, G. Ferreres, D. Hinojosa-Caballero, M. Gutiérrez-Capitán, A. Baldi, C. Fernández-Sánchez, T. Tzanov, Rapid colorimetric detection of wound infection with a fluidic paper device, Int. J. Mol. Sci. 23 (2022) 9129, https://doi.org/10.3390/ijms23169129.

Víctor Pérez-Ginés is a PhD student in the Chemistry Faculty at the Complutense University of Madrid, and since 2021, he is a member of the Electroanalysis and Electrochemical (Bio) Sensors research Group (GEBE-UCM). His current research is mainly focused on the rationale design and development of electrochemical-transduced based biosensing devices with promising applications for the diagnosis and prognosis of high-impact emerging diseases.

David Valero-Calvo received his BSc in Chemistry in 2020 at the University of Cádiz (Spain). He is now a PhD student in the NanoBioAnalysis group, Department of Physical and Analytical Chemistry, University of Oviedo (Spain) under a Pre-doctoral Researcher (FPI) grant. His research interests focus on the development of biosensors based on nanomaterials for the detection of biomarkers of clinical interest for diagnosis.

Rebeca M. Torrente-Rodríguez is Assistant Professor in the Department of Analytical Chemistry at the Faculty of Chemical Sciences of the Complutense University of Madrid. Her research career in the "Electroanalysis and Electrochemical (Bio)sensors" Group (GEBE-UCM) is focused on the design, development and implementation of electro-analytical biosensing devices applicable to the individual and n-plex interrogation of clinically relevant biomarkers at different omic levels in samples of varied origin and nature.

María Pedrero is Assistant Professor at the Department of Analytical Chemistry of the Faculty of Chemical Sciences at the Complutense University of Madrid since 2002. She is a member of the "Electroanalysis and Electrochemical (Bio)sensors" Research Group (GEBE-UCM). Her research area includes the development and study of electrochemical (bio)sensors for the determination of proteins and oligonucleotides as markers of cancer and cardiovascular and neurological diseases. She is co-author of 128 journal articles (97 research articles and 31 review articles) and 13 book chapters on Analytical Electrochemistry, Sensors and Biosensors in Analytical Chemistry.

Francisco Javier García-Alonso received his PhD in Chemical Sciences in 1982 from the University of Valladolid (Spain). He is Full Professor in Inorganic Chemistry at the University of Oviedo (Spain) since 2009. His research interests focus on the synthesis of novel inorganic nanomaterials for applications in biosensing.

José M. Pingarrón is Full Professor of Analytical Chemistry, founder and current member of the group "Electroanalysis and electrochemical (bio)sensors" (GEBE-UCM) at the Complutense University of Madrid. His lines of research include the development of nanostructured electrochemical platforms (enzymatic sensors, immunosensors and genosensors) for the simple or multiplexed determination of relevant biomarkers. He is an honorary advisory member of the journal Electroanalysis and since 2017 a "Fellow" of the International Society of Electrochemistry.

Susana Campuzano is Full Professor in the Department of Analytical Chemistry at the Faculty of Chemistry of the Complutense University of Madrid (Spain) and Director of the Research Group "Electroanalysis and Electrochemical (Bio) Sensors" (GEBE-UCM). Her areas of interest include the development of affinity-based electroanalytical biotechnologies with potential for multiplexed and/or multi-omic determinations in precision healthcare. She is an associate editor of the journal Electroanalysis (Wiley-VCH).

Alfredo de la Escosura-Muñiz holds a PhD in Chemistry (2006) from the University of Oviedo (Spain). As of December 2023, he holds a position as Associate Professor in the Nanobioanalysis Group, Department of Physical and Analytical Chemistry, University of Oviedo (Spain). His research interests focus on the development of biosensing systems based on nanoparticles and nanochannels for point-of-care diagnostic applications.